Article

Chinese Science Bulletin

Geophysics

November 2013 Vol.58 No.33: 4126–4132
doi: 10.1007/s11434-013-5764-8

# Plasma transport between the ionosphere and plasmasphere in response to solar wind dynamic pressure pulsation

ZHANG QingMei[1,2*], WANG Chi[2,1*], LI Hui[2] & LI ChuanQi[1,3]

[1] *College of Math and Statistics, Nanjing University of Information Science and Technology, Nanjing 210044, China;*
[2] *State Key Laboratory of Space Weather, Center for Space Science and Applied Research, Chinese Academy of Sciences, Beijing 100190, China;*
[3] *College of Electronic Engineering, Guangxi Normal University, Guilin 541004, China*

Received December10, 2012; accepted February 7, 2013; published online June 24, 2013

The plasma transport between the plasmasphere and the ionosphere in response to the interplanetary conditions is still not fully understood until now. Simultaneous observations of the plasmasphere and ionosphere from the newly developed Chinese Meridian Project provide a new opportunity for understanding the characteristic of the plasma transport and the coupling mechanism between these two regions. We investigate the response of the plasmasphere ($L \approx 2$) and ionosphere to the solar wind dynamic pressure pulse during geomagnetically quiet period of 21–27 March 2011. The response of the plasmasphere shows a significant depletion. The plasmaspheric density nearly decreases by half in response to the solar wind dynamic pressure pulse, and subsequently recovers to the original level in 1–2 d. Meanwhile, the maximum electron density of the ionospheric F2 layer (NmF2) and the total electron content (TEC) increase by 13% and 21%, respectively, and then gradually recover, which is opposite to the behavior during magnetic storms. Preliminary analysis shows that the plasmaspheric depletion may be mainly caused by the southward interplanetary magnetic field and changing dawn-dusk electric field. The plasmaspheric density variations seem to be controlled by both the IMF and ionospheric conditions.

**solar wind dynamic pressure, ionosphere, plasmasphere, southward IMF, dawn-dusk electric field**

**Citation:** Zhang Q M, Wang C, Li H, et al. Plasma transport between the ionosphere and plasmasphere in response to solar wind dynamic pressure pulsation. Chin Sci Bull, 2013, 58: 4126–4132, doi: 10.1007/s11434-013-5764-8

Geospace which consists of solar wind, magnetosphere and ionosphere is a complex coupling system. The mass exchange between these regions is one important physical process. How does it respond to the variations of solar wind and geomagnetic conditions is a fundamental issue in space physics.

Understanding the relationship between the variations of the magnetospheric plasma density and ionospheric electron density has been an important topic since the 1960s. Using the ducted whistlers observations, Carpenter [1] showed that the inner magnetospheric electron density at the radial distance (about 2–4 $R_E$) has been affected by the intensity of the severe magnetic storms. Chi et al. [2], analyzed the decreases of the plasmaspheric density at $L \approx 2$ and the ionospheric electron density during magnetic storms simultaneously observed by the ground-based stations and global positioning system (GPS) monitors. They suggested that the plasmaspheric depletion was caused by the strong electric field convection of the magnetopause. Additionally, Chi et al. [3] also showed that the ionosphere importantly regulated the variation of magnetospheric plasma density based on the prominent increases of the inner magnetospheric plasma density ($L \leqslant 4$) and the ionospheric electron density at local afternoon sector during the 2003 Halloween magnetic storm. Similarly, a reduction of the outer magnetospheric plasma density ($4 \leqslant L \leqslant 8.5$) was due to a strong convection of the magnetosphere and the ionosphere. Recently, Wang et al. [4] found the reduction of the ionospheric electron density occurred before the plasmaspheric density reached its minimum using the data from MHT geomagnetic station in 2011

*Corresponding authors (email: qmzhang@spaceweather.ac.cn; cw@spaceweather.ac.cn)

in the meridian chain of comprehensive ground-based space environment monitors in the eastern hemisphere (or Chinese Meridian Project for short) [5]. Therefore, they suggested that the plasmaspheric depletion was very likely due to the reduced plasma supply from the ionosphere and the plasmaspheric dynamics seemed to be controlled by the ionosphere. Spasojevic and Sandel [6] analyzed the data from the Extreme Ultraviolet (EUV) imager on the IMAGE satellite Images and concluded that the loss rate of the plasmaspheric $He^+$ ions varied with the interplanetary dawn-dusk electric field $E_y$, and was correlated with the duration of strongly positive interplanetary dawn-dusk electric field $E_y$ when it was stronger than 2.5 mV/m during a weak geomagnetic disturbance interval. Generally speaking, the southward interplanetary magnetic field (IMF *Bz*) mainly triggered the geomagnetic storm. As an important type of all kinds of interplanetary disturbances, solar wind dynamic pressure pulsations affect the coupling between the solar wind-magnetosphere-ionosphere system. However the plasmas transport between those regions is still controversial in space physics. Guo et al. [7] analyzed the correlation of ions densities such as $O^+$, $H^+$ and $He^+$ in cusp region with solar wind dynamic pressure and geomagnetic *Kp* index. They found that these ions densities had a strong positive correlation with solar wind dynamic pressure. To further explore the controlling factors of plasmaspheric density and the plasma transport process between the magnetosphere and the ionosphere, we use the data from the ground-based station of the newly developed Chinese Meridian Project and investigate the plasma transport process in response to the single solar wind dynamic pressure pulsation during a geomagnetically quite period.

The Chinese Meridian Project is a near-Earth space environment monitoring network. It consists of 15 ground-based observatories located roughly along the 120°E geographic longitude meridian and the 30°N geographic latitude. Each observatory is equipped with multiple instruments such as radio instruments, magnetometers, optics and sounding rocket to continuously monitor the space environment from the middle-upper atmosphere (20–30 to hundreds of km from the Earth surface), ionosphere and magnetosphere, and up to the interplanetary space. With simultaneous observations of the geomagnetic field and ionosphere, the Chinese Meridian Project provides an excellent opportunity to explore the plasma transport and the coupling process between the magnetosphere and ionosphere.

In this study, we investigate the variations of the equatorial plasma density in the plasmasphere ($L \approx 2$) in response to solar wind dynamic pressure pulsation using the geomagnetic field data from the Chinese Meridian Project. Meanwhile, with the total electron content (TEC) inferred from GPS monitor and the ionosphere F2 layer critical frequency foF2 from the digisonde, we estimate the ionospheric electron density, and further analyze the plasma transport between the plasmasphere and ionosphere in response to the solar wind pressure pulsation.

## 1 Methodology

Using the geomagnetic field data from the Chinese Meridian Project, we calculate the equatorial plasma density in the plasmasphere from the ultra low frequency waves (ULF) sensing the magnetic field line resonance (FLR). In order to obtain the plasma density, the resonance signals of the magnetic field have been identified to calculate the oscillating eigenfrequency of a specified magnetic field line. We use both the gradient technique (Baransky et al. [8]) and the cross-phase method (Waters et al. [9] and Kawano et al. [10]) to obtain the resonance frequency of the resonating magnetic field line midway between the two closely spaced stations at specific latitudes from the dynamic spectra of the phase difference and power density ratio of the *H* component. Waters et al. [9,11] first applied the cross-phase method to obtain the clear phase difference spectrum. The cross-phase technique is based on the principle that the phase difference of FLR of the *H* component observed by two closely spaced stations located along the same longitude maximizes at the eigenfrequencies of the field line midway between the two stations. As for the gradient method, the resonant frequency ($f_R$) is estimated from the dynamic power spectrum of the *H* component for the resonating magnetic field line whose foot point is halfway between the two stations and contents the requirement of the power density ratio passing through near unity ($\log(1) = 0$), while the errors in FLR are 3–5 mHz [12]. It is found that the eigenfrequency of the fundamental mode of field line resonances is in the Pc3 frequency range (22–100 mHz) at mid- and low-latitudes.

The resonant frequency depends on the length of the magnetic field line, the strength of the geomagnetic field and the plasma density along the magnetic field line. The plasma mass density can be then inferred from the observed eigenfrequency if the appropriate models of the magnetic field and the plasma density are utilized. At mid- and low-latitude regions, we choose the dipole magnetic field model because of the closed magnetic field lines. The plasma density $\rho$ can be estimated as $\rho \propto r^{-m}$, where $r$ is the geocentric radial distance from the Earth center and m is the plasma density index. In particular, for this range of latitudes ($1.8 < L < 2.2$), an index m in the range of 0–2 may be appropriate [14] and the inferred equatorial plasmaspheric density $\rho_0$ is not sensitive to the particular choice of m within this range, so we choose the index $m = 1$ in our calculation. Furthermore, the equatorial plasma density $\rho_0$ also follows $\rho_0 \propto (f_R)^{-2}$ with $f_R$ along the magnetic field line at a special latitude.

Using the data of fluxgate magnetometers equipped at the ground geomagnetic stations Mohe (MHT) and Man-

zhouli (MZL), we estimate the fundamental mode frequency of the resonant frequencies of Pc3 geomagnetic pulsation and further use it to invert the plasma densities. The fluxgate magnetometers at these stations record the geomagnetic *H*, *D* and *Z* components. The sample rate is 1 Hz and the noise level of the systems is about 0.1 nT. The locations of the stations MHT and MZL are listed in Table 1. The resonance point halfway between the two stations has an *L* value approximately equal to 2.14. At the same time, the digisonde at MHT gives 15-min time resolution of the foF2 values, and TEC monitor provides 30-s time-resolution data. The 1-min OMNI data of the solar wind plasma parameters and interplanetary magnetic field from March 21 to March 27 are obtained from the CDAWeb website.

## 2 Event analyses

A single solar wind dynamic pressure pulsation event during a relative geomagnetically quiet (SYM-H $\geqslant$ –30 nT) period (5–7 d) in 2011 should be first identified from the solar wind data of OMNI data on the CDAWeb website. We required that the value of the solar wind dynamic pressure should sharply increase more than twice of the initial value. And there should have simultaneous observations of the geomagnetic field data from the fluxgate magnetometers at MHT and MZL and of the ionospheric data from the digisonde and GPS monitors at MHT. Under these selection criteria, one solar wind dynamic pressure pulsation event from March 21 to March 27 was identified. The corresponding solar wind observations are shown in Figure 1. From the top to bottom, the panels present the three components of the interplanetary magnetic field in GSE coordinate, the magnetic field intensity, solar wind speed, solar wind dynamic pressure, solar wind proton number density, solar wind electric field and the symmetry changing magnetic field index SYM-H (high time resolution *Dst* index) of the geomagnetic field *H* component, respectively. The value of solar wind dynamic pressure sharply increases three times from 2.52 nPa at 0515 UT (Universal Time) to 7.43 nPa at 1018 UT on March 22, 2011, and then rapidly decreases to 3.03 nPa at 1100 UT. During this period, the interplanetary magnetic field (IMF) $B_z$ is northward, and the magnitude of IMF remains steady and starts to increase at the end of the negative dynamic pressure pulsation. The solar wind speed *V* remains invariant about 320 km/s. The solar wind dynamic pressure *Pd* is thus mainly controlled by solar wind number density *N* prominently results in the

**Table 1** Locations of stations

| Stations | Magnetic latitude | Magnetic longitude | Geographic latitude | Geographic longitude | *L* value |
|---|---|---|---|---|---|
| MHT | 48.6 | 195.9 | 53.5 | 122.4 | 2.29 |
| MZL | 44.9 | 191.2 | 49.6 | 117.5 | 1.99 |

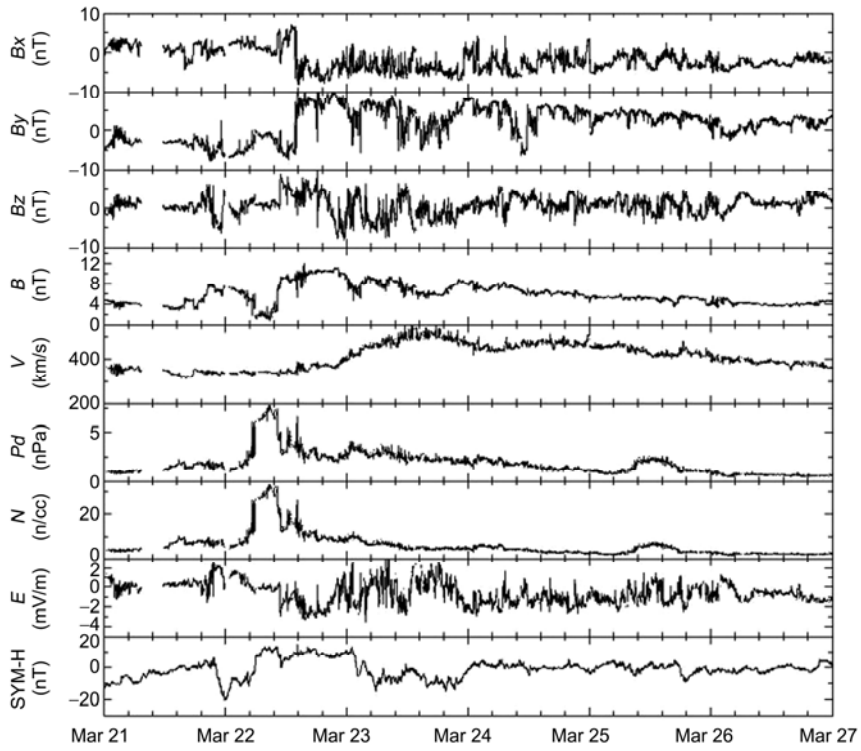


**Figure 1** The solar wind parameters on March 21–27, 2011. From the top to bottom, the panels show three components of the interplanetary magnetic field, the total magnetic field intensity, solar wind speed, solar wind dynamic pressure, solar wind proton number density, the dawn-dusk electric field and geomagnetic index.

variation of the solar wind dynamic pressure. The electric field $E_y$ increases negatively to −2.79 mV/m and the SYM-H index keeps unchanged. Therefore this is a single solar wind dynamic pressure pulsation. On March 23, the southward IMF $B_z$ and the eastward electric field $E_y$ dominate in the interval. During the whole interval, the absolute value of the SYM-H index is less than 20 nT, which suggests a geomagnetically quiet period. The solar wind speed $V$ slowly increases to 542 km/s and then gradually decreases to about 320 km/s. The IMF $B_z$ fluctuates between southward and the northward. The magnetic field intensity decreases and then recovers to the initial value after the next solar wind dynamic pressure pulsation around the end of March 23. The other interplanetary parameters remained basically unchanged.

Figure 2 shows the phase difference spectrum, log power-ratio spectrum and coherence spectrum of the $H$ component at MHT and MZL during March 21–24, 2011, where LT = UT + 8. In the top panel ((a)–(d)), the red-yellow region of the magnetic field line resonance indicates a large phase difference in the phase difference spectrum. In the middle panel ((a)–(d)), the appearance of the bipolar pattern in the bright region of the log power-ratio spectrum suggests the FLR signals at the two stations, respectively. And the resonant frequencies of the field line resonances decrease as the geomagnetic latitude increases [9]. Additionally, the middle region is also the resonance signals region of the field line midway between the two stations. In the bottom panel ((a)–(d)), the bright color corresponds to a large coherence.

It can be seen that the FLR signals can be observed in a short time period during 0000–1000 UT (0800–1800 LT) every day. This is because that Pc3 waves (22–100 mHz) of ULF fluctuations of the FLR monitored at the ground stations at mid- and low-latitude can be only observed at the dayside. And the fundamental mode eigenfrequencies of field line resonances are in the frequency range at the corresponding geomagnetic latitude.

On March 21, FLR signatures appear obviously. The fundamental mode frequencies at about 30–35 mHz can be clearly identified and it decreases over the interval 0400–0900 UT from the phase difference and log power-ratio spectrum shown in Figure 2. On March 22, FLR signatures occurs again and remains stable on the same interval 0400–0900 UT, and the eigenfrequencies of the field line are slightly higher than that on the same time (0600 UT) in the previous day. Meanwhile, the bipolar pattern [9] identifies from the log power-ratio spectrum indicates the eigenfrequencies of the FLR decreases as the geomagnetic

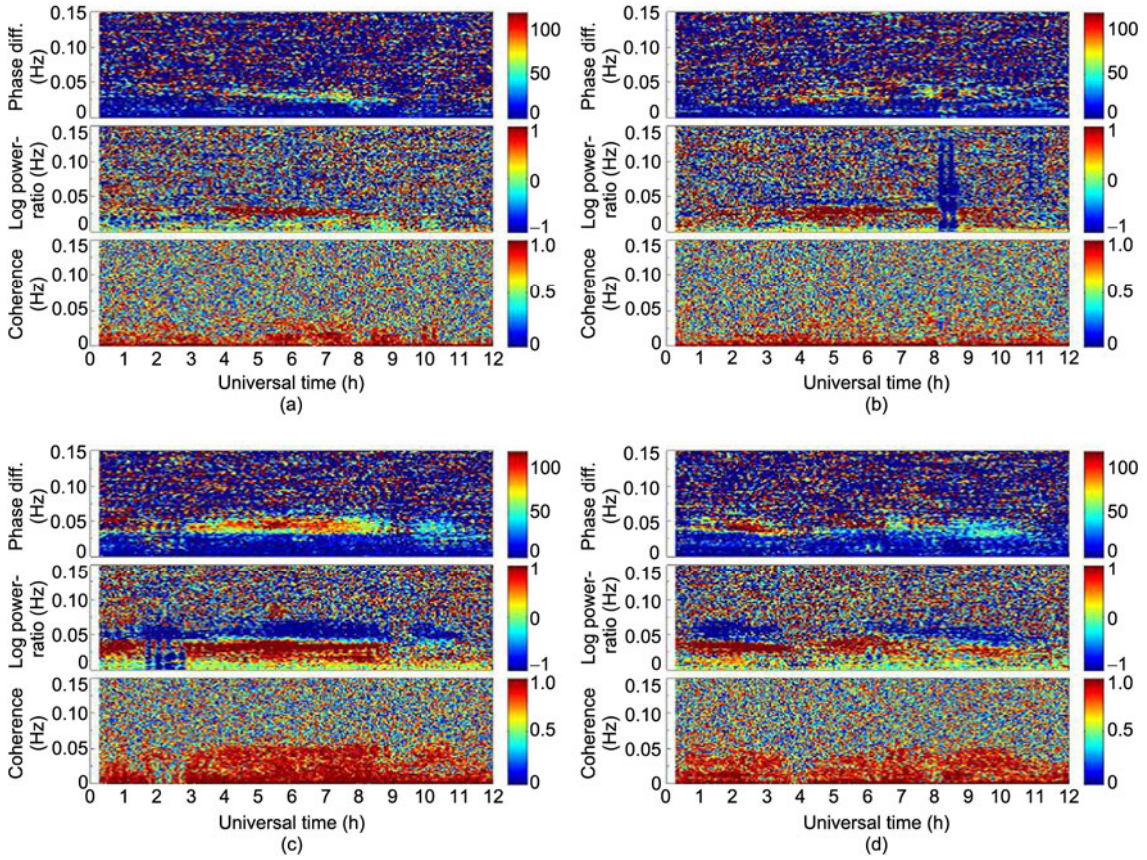


**Figure 2** Phase difference and log power-ratio and coherence spectrograms of the $H$ component for the station pair MHT-MZL. Each diagram shows the spectrogram for the local time interval 0800-2000 during March 21–24, 2011. (a) March 21; (b) March 22; (c) March 23; (d) March 24.

latitudes increase [10] because of the log power value at the higher latitude is corresponding to the lower resonance frequencies. On March 23, FLR signatures are prominent obviously at the dayside, and the fundamental mode eigenfrequencies of field line resonances are almost at 40–50 mHz and more higher than that of during the previous day. It reaches the day before, and even at 46 mHz at 0600 UT in the phase difference spectrum. Similarly, the bipolar pattern observes a larger coherence in the log power-ratio spectrum and an enhanced power shows the larger power of the FLR. On March 24, FLR signatures are weaker than that in the previous day and show the clear bipolar pattern. The fundamental mode eigenfrequency of the FLR is about 47 mHz at 0600 UT. On the following days of March 25–26 (not shown), the fundamental mode frequency is also evident, and the eigenfrequency slowly declines and is close to 30 mHz at 0600 UT on March 21.

The *Dst* index shown in the first panel of Figure 3 (http://wdc.kugi.kyoto-u.ac.jp/index.html) is greater than –20 nT in this interval, which suggests this is a geomagnetically quiet period. The second panel of Figure 3 shows the solar wind speed. It increases to 542 km/s and then declines to 320 km/s after March 23. The third panel of Figure 3 gives the solar wind dynamic pressure. There is a single dynamic pressure pulsation event occurring on March 22. The phase-difference spectrograms have been examined from March 21 to March 27. The fundamental mode eigenfrequencies of the magnetic field line resonances, which are compared with that from the log power-ratio spectrograms and 3–5 mHz difference for the local time 1400 LT (0600 UT), are given in the fourth panel of Figure 3. Similarly, the eigenfrequency increases to the maximum after the solar wind dynamic pressure pulsation and then decreases and recovers to the origin value on March 21, which may be caused by the disturbed geomagnetic environment in response to the strengthened FLRs made by the solar wind dynamic pressure pulsation. Additionally, the error bar indicates the standard deviation of all the eigenfrequency values identified at intervals of one hour during the day.

The fifth panel of Figure 3 gives the equatorial plasma mass density at $L \approx 2$ for the local time 1400 LT (0600 UT). The plasma density decreases to 56% of the original value and to the lowest value on March 21 before the dynamic pressure pulsation, then gradually increases and recovers to the initial value in about 1–2 d. After that, IMF $B_z$ and the electric field $E_y$ remains basically invariant, and during the same period the plasmapheric density gradually increases and recovers to the initial value to refill the plasmasphere. However, the depletion of the plasmasphere occurs during the period the solar wind speed rapidly increases.

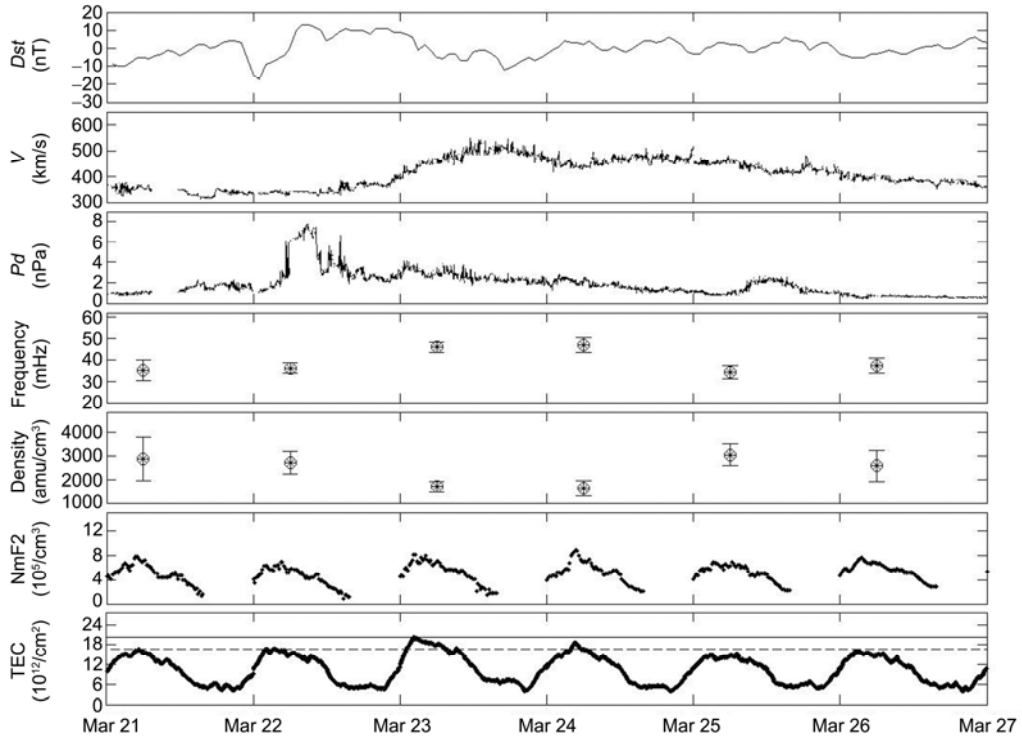


**Figure 3** The plots of the solar wind parameters, eigenfrequencies and ions densities on March 21–27, 2011. From the top to bottom panels shown *Dst* index, solar wind speed, solar wind dynamic pressure, fundamental mode frequencies of field line resonances at $L \approx 2$ for the local time 1400 (0600 UT), equatorial plasma mass densities, the ionospheric F2 layer maximum electron density values (NmF2) and the total electron content (TEC) values during geomagnetically quiet period of March 21–27, 2011. The solid line and dashed line in the last panel indicate the peak value on March 21 and the maximum TEC daily peak value on March 23, respectively.

The bottom two panels of Figure 3 show the NmF2 value from the digisonde and the vertical TEC value from GPS measurements above MHT. As can be seen in the two panels present the highest values in the early afternoon and the lowest values just before sunrise. Unlike the variation of the plasma density, the increases of the daily NmF2 and TEC peak values by approximately 13% and 22%, respectively, occur after the dynamic pressure pulsation and rise to the highest values, and then a reduction of the peak values by 14% and 21% recovers to the initial value on March 21. The daily NmF2 and TEC peak values increase slightly after the solar wind dynamic pressure pulsation, which are distinctly different from that decreases before the plasmaspheric density drops during magnetic storms.

## 3 Summary and discussion

In this paper, we obtained the fundamental mode eigenfrequency of the FLR by applying both the phase difference and log power-ratio technique to the magnetometer data from two ground stations of the Chinese Meridian Project. Moreover, under the assumptions of the dipole magnetic field and plasma density model, we examined the variation of the plasmaspheric density in response to a solar wind dynamic pressure pulsation during geomagnetically quiet period of March 21–27, 2011. The equatorial plasma density at $L \approx 2$ nearly decreased by roughly 50% in response to the solar wind dynamic pressure pulse, and then recovered to the initial value. Additionally, the electron density of the ionosphere increased and then gradually recovered to the original level, which is a typical case of plasmasphere depletion in response to the solar wind dynamic pressure pulsation during a geomagnetically quiet period. This result is consistent with the findings that the plasmaspheric density decreased at mid- and low-latitude during the magnetic storm proposed by Chi et al. [2] and Villante et al. [15] and our previous result that showed a corresponding decrease of the plasmaspheric density during moderate magnetic storm events in 2011.

To roughly estimate the location of the plasmasphere for the solar wind dynamic pressure pulsation event, we employ the empirical formula of the plasmaspause location Lpp from spacecraft and whistler observations at higher L-shells [16]. The plasmaspause location Lpp increased from 4.2 to 4.8 after the coming of the solar wind dynamic pressure pulsation event (*Kp* from 3+ to 2–). The plasmaspause never came inside of $L \approx 2$ for this event. This indicates that the decrease of the plasmaspheric density at this L value is unlikely due to the motion of the plasmaspause in this case. After the solar wind dynamic pressure pulsation event, we notice that there existed continuous variations of southward IMF $B_z$ and significant changes of the solar wind electric field $E_y$, which may lead to the decrease of the plamaspheric density. In addition, the enhanced magnetospheric convection caused by the solar wind electric field $E_y$ makes the plasma drifting toward the magnetospheric boundary layer on the dayside ionosphere and thus the plasmaspheric density induction. This result is similar to the conclusion made by Spasojevic [6] that the loss rate of the plasmaspheric $He^+$ ions by EUV Image measurements is correlated with the amplitude of the interplanetary electric field $E_y$ during the disturbed geomagnetic period. While the increases of the inonspheric electron density in response to the solar wind dynamic pressure may be caused by the uplifting of the F layer through the $\boldsymbol{E}\times\boldsymbol{B}$ drift, which is the curl of the dawn-dusk interplanetary electric field and the proximate horizontal magnetic field, as the solar wind speed increases. When the southward IMF $B_z$ and dawn-dusk electric field $E_y$ change abruptly and recover gradually, the decrease of the ionospheric TEC peaks is before the increases of the plasmaspheric density. As a result, the ionospheric ions transport to the plasmasphere along the magnetic flux tube leads to the increase of the plasmaspheric density and then recovers to the origin value. A similar finding might be responsible for the refilling of the plasmasphere during the recovery phase of the magnetic storm studied by Wang et al. [4]. After the solar wind dynamic pressure pulsation, the plasmaspheric density increased by 88% of the minimum value and recovers to a slightly higher level than the initial value, while the ionospheric electron density decreases by 21% of the maximum and recovered to the original level, and then the increment is greater than the decrement. These results suggest that a minor change in the ionospheric TEC may result in a significant impact on the plasmaspheric density. So these findings show the plasmaspheric depletion may be mainly caused by the southward IMF $B_z$ and changing $E_y$ in response to the solar wind dynamic pressure pulsation, and the plasmaspheric refilling is a result of the decrease of the ionospheric density. The plasmaspheric density thus seems to be controlled by both the IMF and ionospheric conditions.

The decreases of the plasmapheric density and the daily NmF2 and TEC peak values do not depend on the strength of the solar wind dynamic pressure pulsation at $L \approx 2$. However, we need to investigate more events with different intensity to make reliable conclusions in the future.

In conclusion, using the data of fluxgate magnetometers from the data center of the Chinese Meridian Project to analysis simultaneously the equatorial plasmaspheric density and the ionospheric TEC, the plasmaspheric density decreases for both the magnetic storm event and the solar wind dynamic pressure pulsation event. However, the variation of NmF2 and TEC in response to this solar wind dynamic pressure pulsation event are different from that those during magnetic storms. During magnetic storm events, the plasmaspheric depletion is probably due to the reduced plasma supply from the ionosphere, while during this solar wind dynamic pressure pulsation event the plasmaspheric refilling may result from the ionospheric ions drift into the

plasmasphere along the upward magnetic tubes. These results indicate the important roles of the interplanetary condition and the ionosphere in controlling of the plasma transport and the dynamic process of the plasmasphere.

*We acknowledge the use of geomagnetic field data and GPS data from the geomagnetic field observatories of Chinese Meridian Project, and the solar wind plasma and interplanetary magnetic field data from OMNI Data Center provided by NASA CEAWEB. We thank H. Shen for help with TEC calculations. This work was supported by the National Basic Research Program of China (2012CB825602), the National Natural Science Foundation of China (41231067 and 41204118) and in part by the Specialized Research Fund for State Key Laboratories of China.*

1 Carpenter D L. Electron-Density variations in the Magnetosphere Deduced from Whistler Data. J Geophys Res, 1962, 67: 3345–3360
2 Chi P J, Russell C T, Musman S, et al. Plasmaspheric depletion and refilling associated with the September 25, 1998 magnetic storm observed by ground magnetometers at $L = 2$. Geophys Res Lett, 2000, 27: 633–636
3 Chi P J, Russell C T, Foster J C, et al. Density enhancement in plasmasphere-ionosphere plasma during the 2003 Halloween Superstorm: Observations along the 330th magnetic meridian in North America. Geophys Res Lett, 2005, 32: L03S07
4 Wang C, Zhang Q M, Chi P J, et al. Simultaneous observations of plasmaspheric and ionospheric variations during magnetic storms in 2011: First result from Chinese Meridian Project. J Geophys Res, 2013, 118: 1–6
5 Wang C. New chains of space weather monitoring stations in China. Space Weather, 2010, 8: S08001
6 Spasojevic M, Sandel B R. Global estimates of plasmaspheric losses during moderate disturbance intervals. Ann Geophys, 2010, 28: 27–36
7 Guo J G, Shi J K, Zhang T L, et al. The correlations of ions density with geomagnetic activity and solar dynamic pressure in cusp region. Chin Sci Bull, 2007, 52: 967–971
8 Baransky L N, Borovkov J E, Gokhberg M B, et al. High resolution method of direct measurement of the magnetic field lines' eigenfrequencies. Planet Space Sci, 1985, 33: 1369–1374
9 Waters C L, Menk F W, Fraser B J. The resonance structure of low latitude Pc3 geomagnetic pulsations. Geophys Res Lett, 1991, 18: 2293–2296
10 Kawano H, Yumoto K, Pilipenko V A, et al. Using two ground stations to identify magnetospheric field line eigenfrequency as a continuous function of ground latitude. J Geophys Res, 2002, 107: 251–262
11 Waters C L, Menk F W, Fraser B J. Low latitude geomagnetic field line resonance: Experiment and modeling. J Geophys Res, 1994, 99: 17547–17558
12 Berube D, Moldwin M B, Fung S F, et al. A plasmaspheric mass density model and constraints on its heavy ion concentration. J Geophys Res, 2005, 110: A04212
13 Schulz M. Eigenfrequencies of geomagnetic field lines and implications for plasma-density modeling. J Geophys Res, 1996, 101: 17385–17397
14 Vellante M, Förster M. Inference of the magnetospheric plasma mass density from field line resonances: A test using a plasmasphere model. J Geophys Res, 2006, 111: A11204
15 Villante U, Vellante M, Francial P, et al. ULF fluctuations of the geomagnetic field and ionospheric sounding measurements at low latitudes during the first CAWSES campaign. Ann Geophys, 2006, 24: 1455–1468
16 Carpenter D L. An ISEE whistler model of equatorial electron density in the magnetosphere. J Geophys Res, 1992, 97: 1097–1108